Swelling of Ionic and Non-Ionic Surfactant Micelles by High Pressure Gases

John M. O' Callaghan, Hugh McNamara[α], Mark P. Copley, John P. Hanrahan, Michael A. Morris, David C. Steytler[#], Richard K. Heenan[†] and Justin D. Holmes[*]

Materials and Supercritical Fluids Group , Department of Chemistry and the Tyndall National Institute, University College Cork, Cork, Ireland and the Centre for Research on Adaptive Nanostructures and Nanodevices (CRANN), Trinity College Dublin, Dublin, Ireland. [α]Department of Applied Mathematics, University College Cork, Cork, Ireland. [#]School of Chemical Sciences and Pharmacy, University of East Anglia, Norwich, NR4 7TJ, UK. [†]ISIS-CLRC, Rutherford Appleton Laboratory, Chilton, Oxfordshire, OX110QX, UK.

* To whom correspondence should be addressed: Tel: +353(0)21 4903301; Fax: +353 (0)21 4274097; E-mail: j.holmes@ucc.ie

Abstract

The influence of different solvent environments on the size, shape and characteristics of surfactant micelles of Pluronic F127 and CTAB was investigated by small angle neutron scattering (SANS). SANS experiments were undertaken on dilute micellar surfactant solutions of F127 and CTAB which between them were exposed to liquid and supercritical carbon dioxide, liquid propane, ethane and heptane under various pressures and temperatures. Swelling of the surfactant micelles could be directly related to the solubility of the solvents within the micelles, especially within their cores. Carbon dioxide produced the largest swelling of the Pluronic F127 micelles, compared to propane and ethane, which mirrors the solubility of the gases in the PPO core of the micelles. Conversely, the extent of swelling of the cores of CTAB micelles was greater with propane compared to carbon dioxide, which again relates to the solubility of the solvents in the alkane core of the CTAB micelles.

Introduction

Pluronic amphiphilic block copolymers are used extensively in a wide range of applications, including detergents[1-2], separations[3-4], drug solubilisation and delivery[5-7] and the controlled release of drugs[8-10]. As a result there have been a significant number of small angle scattering studies on the structural properties of non-ionic Pluronic surfactants, especially in low concentration aqueous environments, including a number of review articles[11-12]. One of the first structural studies of Pluronic surfactants was conducted by Zhou *et al.*[13] who used dynamic light scattering to investigate the structure and assembly of micelles. Since then a lot of research has been conducted into probing the structural characteristics of copolymer micelles using small angle scattering techniques[14-17]. The ionic surfactant cetyltrimethylammonium bromide (CTAB)

has also been widely studied because of its use as a template in the synthesis of mesoporous silicas[18-19], as a detergent[1], in the stabilization of nanoparticles[20-21] and also in separation science[22]. The structure properties of CTAB micelles in various systems have been extensively studied using small angle neutron scattering (SANS) techniques; see Aswal *et al.*[23-24].

A characteristic of many micelle systems is their ability to take up large amounts of a suitable solvent and consequently swell in size. There have been many studies on the solubilisation of various hydrocarbons, alcohols and other additives in micellar systems and the consequential swelling of the micelles by their addition. For example, Hai *et al.*[25] reported the solubilisation of pentane in micellar solutions of sodium dodecyl sulphate and Chaiko *et al.*[26] also measured the solubility of a number of hydrocarbons in different micellar solutions, demonstrating that the size and polarity of hydrocarbons affected their solubilisation within the structure of surfactant micelles. Ma *et al.*[27] investigated the micellisation of the Pluronic P85 in the presence of different oils; where they discovered a temperature dependence of the critical micelle concentration, which decreased with increasing oil concentration. The core of the micelles was also observed to swell significantly at low oil concentrations. ChilluraMartino *et al.*[28] showed the versatility of SANS to investigate the structures of various polymers, such as (poly(1,1-dihydroperfluorooctyl acrylate), poly(hexafluoropropylene oxide) and poly(dimethyl siloxane)), in supercritical carbon dioxide. Friman *et al.*[29] used small angle x-ray scattering to investigate the micellisation of sodium octanoate in the presence of octane-1,8-diol, which was found to penetrate into the hydrocarbon core of the micelles causing them to swell considerable. SANS determination of the temperature induced swelling of high concentrations of F127 micellar solutions has also been reported by Lenaerts *et al.*[30]. Liu *et al.*[31] investigated the effects of

compressed carbon dioxide on reverse micelles of AOT and observed that the solubility of carbon dioxide in the micelles changed as a function of pressure. Hakoda *et al.*[32] reported that supercritical ethane had no influence on the diameter of lipase-containing reversed AOT micelles.

Swollen micelles can also be employed to produce a material with the inverse structure of the micelle system itself, such as mesoporous silica. For example, Cao *et al.*[33] enlarged the pores of SBA-15 mesoporous silica templated from Pluronic P123 by adding 1,3,5-triethylbenzene and 1,3,5-triisopropylbenzene during the synthesis process. Ruggles *et al.*[34] investigated the changing unit cell dimensions of a 2-dimensional hexagonal mesoporous silica thin film, templated from CTACl and CTABr micelles, after the addition of high molecular weight hydrocarbons (C_8 to C_{16}) during synthesis. Zhou *et al.*[35] also used a micellar system loaded with 1,3,5-trimethylbenzene to produce cubic periodic mesoporous organosilica which possessed enlarged pores diameters. Causse *et al.*[36] showed that tributylphosphate was able to swell a number of Pluronic surfactant solutions used to make mesoporous silica materials due to its affinity for the hydrophobic core of the micelles. The addition of trimethylbenzene during the synthesis of mesoporous silica was also seen to result in material with enlarged pores, as reported by Chen *et al.*[37]. The addition of the swelling agent triisopropyl benzene during the synthesis of CTAB-templated mesoporous silica resulted in swollen 2-dimensional hexagonal system as reported by Fukuoka *et al.*[38]. With increasing amounts of triisopropyl benzene during the synthesis a phase change from 2-dimensional hexagonal to a cubic system was observed. Blin *et al.* [39] studied the affect of alkane addition on the synthesis a of CTAB-templated mesoporous silicas; decane was found to be the most successful swelling agent of CTAB in that study.

Similarly to the work on mesoporous materials, O'Driscoll *et al.*[40] used SANS measurements to determine the mesostructure of CTAB/polyethylenimine polymer films after the incorporation of small organic molecules. Cyclohexane and decane was observed to homogeneously swell the structure of the films and swelling of the prolate elliptical CTAB micelles by cyclohexane extended the main axis of the micelles.

We have previously demonstrated the swelling of liquid crystal films[41] during the synthesis of mesoporous silica[42] using supercritical carbon dioxide (sc-CO_2). This work has stimulated us to conduct a more detailed study on the changing micelle dimensions of F127 and CTAB micelles with increasing pressures of liquid and supercritical carbon dioxide, propane and ethane. Here we report how dilute Pluronic F127 and CTAB micellar solutions swell when exposed to different solvents, as a function of temperature and pressure. SANS analysis was used to determine the changing size, shape and composition of the micelles and their interactions with neighboring micelles during the swelling process.

Experimental

Materials and Reagents. Cetyltrimethylammonium bromide (CTAB) was used as received from Fluka, UK and the polyethylene oxide-polypropylene oxide- polyethylene oxide triblock copolymer Pluronic F127 ($PEO_{100}PPO_{65}PEO_{100}$), was used as received from BASF, New Jersey, U.S.A. Deuterium oxide (D_2O) was used as supplied by Sigma-Aldrich. Carbon dioxide (99.8 %), ethane (99.97 %), propane (99.97 %) gases and heptane (anhydrous 99 %) were also supplied by Sigma-Aldrich.

SANS Measurements on Micellar Solutions. *In-situ* high-pressure SANS experiments were conducted on the LOQ instrument at ISIS at the Rutherford Appleton Laboratory (RAL) in Oxfordshire, UK. The absolute scattering cross-section I(Q) (cm^{-1}) was measured as a function of the modulus of momentum transfer $Q(A^{-1}) = (4\pi/\lambda) \sin(\theta/2)$ where λ is the incident neutron wavelength (2.2 to 10 Å) and θ is the scattering angle (< 7°). All measurements were conducted at 40 °C. High pressure SANS measurements were made using the UEA high pressure cell which is described in detail elsewhere[43]. Measurements performed on surfactant/D_2O mixtures were conducted at surfactant concentrations of 2.5 wt%. The critical points of carbon dioxide are 31° C and 7.15 MPa[44], those of propane are 96.6° C and 4.25 MPa[45] and of ethane are 32.2° C and 4.82 MPa[45]. The critical points of heptane are 267.2° C and 2.74 MPa[46].

A stock solution of the micellar solution, which consisted of 2.5 wt% surfactant (either F127 or CTAB) in D_2O was prepared 2 hr before any SANS measurements were conducted. The surfactant was dissolved in D_2O while stirring at room temperature before being placing in the high pressure cell. The high pressure cell and aqueous micellar solution were allowed to

equilibrate, at both the desired temperature and pressure, for up to 30 min before any SANS data was collected.

Pluronic Fitting Parameters. Many models have been developed to obtain structural data from the scattering of micelle solutions. In this work, Pluronic SANS data was fitted using the model described by Mortensen *et al.*[47]. More recently, this model has been used by Yang *et al.*[48] to investigate the effects of temperature on Pluronic L64 micelles and by Goldmints *et al.*[49] who investigated micelle formation from Pluronic P85. The model is described in full in the supporting information and further background can be found in the above references. A least square fitting routine was used to model the scattering data. The fitted Pluronic micelle parameters were the core radius R_1, the micelle radius R_2, the hard sphere radius R_{HS}, the volume fractions of the core components (PPO, water and swelling solvent) and the micelle volume fraction. The aggregation number of the micelle was calculated from a constant micelle core surface area per F127 molecule.

CTAB Fitting Parameters. The fitting program FISH[50] was used to model the scattering data from CTAB micelles placed under liquid CO_2, supercritical CO_2 (sc-CO_2) and liquid propane environments. The model that was chosen to fit the CTAB data was a Hayter-Penfold charged particle with an elliptical morphology, which is the model of choice when fitting scattering data from CTAB micelles[24, 51] or other charged particle with elliptical shapes[52]. The fitted CTAB micelle parameters were the semi-minor axis of the ellipitical CTAB micelle *a*, the ellipicity of the CTAB micelle *X* and the hard sphere radius R_{HS}. The volume fraction of solvent in the core was estimated from the size increase of the micelle.

Results and Discussion

Swelling of F127 Micelles with Carbon Dioxide. Figure 1(a) shows the fitted SANS data obtained from a CO_2-swollen 2.5wt% F127 aqueous micellar solution as a function of pressure. A significant change was observed in the isotropic micelle scattering as the pressure of CO_2 was increased, at a constant temperature of 40 °C, which can be attributed to (i) an increase in the mean radius of the F127 micelles with increasing CO_2 pressure, (ii) a decrease in the degree of hydration of the micelle core or (iii) an increase in the micellar number density. From our analysis of the SANS data, and previous experience with other Pluronic systems we conclude that the increase in I(Q) intensity is due to an increase in the mean radius of the F127 micelles.

Figure 1(b) shows the micelle core radius (R_1) and micelle radius (R_2) and Figure 1(c) shows the fitted volume fraction of CO_2 in the core of the micelles as a function of pressure, obtained by modelling the SANS data at different sc-CO_2 pressures. Both the core radius (R_1), consisting of PPO groups, and the corona-core-corona radius (R_2), consisting of both PEO and PPO groups, showed an increase with increasing CO_2 pressure. R_1 was observed to increase from a value of 44 Å at atmospheric pressure, to a mean value of 54 Å at 50 MPa.

The swelling profile seen in Figure 1(b) is very similar to data we have published previously for the Pluronic P123 surfactant [41-42], where the swelling of the micelles and liquid crystals is most effective up to approximately 10 MPa after which time the swelling is not as dramatic, even thought the density of CO_2 continues to increase at higher pressure[53]. As we have previously reported[41] micellar swelling is due to the solubility of CO_2 in the Pluronic micelles, more specifically the solubility of CO_2 in the micelle hydrophobic polypropylene oxide (PPO) core,

which is similar to hydrocarbon solubilisation in Pluronic micelles[54]. Figure 1(c) shows the an increase of CO_2 in the micelle core as a function of pressure, which was also observed by Sato *et al.*[55] who reported the solubility of CO_2 in PPO increases with pressure. Comparing the maximum core radius that would result from an untangled all-trans configuration of the PPO_{65} polymer segment (~89 Å), which represents the absolute maximum and thermodynamically improbable radius attainable for a swollen F127 micelle, and the maximum core radii reported here (54 Å) is in reflection, a very rational value.

The corresponding micelle radius (R_2) also increases during the experiment but it is not thought that the PEO block takes part in the swelling process, however the corona thickness is surprising small especially seeing as it is composed of 100 PEO units. The large number of PEO units present in the corona of the micelle results in the interface between the hydrated PEO shell and the D_2O solvent phase being poorly defined, in terms of scattering length densities (SLDs) as say compared to the core-corona interface. The boundary between the PEO corona and the solvent becomes blurred as the PEO chains disperse in the solvent phase, which is consistent with the Pluronic micelle model of a dense PPO core with a highly hydrated PEO corona[12]. This poorly defined interface ultimately results in an inaccurate corona thickness.

The hard sphere S(Q) radius (R_{hs}) is also observed to increase consistently as the pressure increases (data not shown). The micelle volume fraction of the F127 micelles at room pressure and 40° C is in agreement with previous reports on low wt% F127 micellar solutions[56] and is seen to increase from 0.11 to 0.13 during the course of the experiment, which is consistent with the increasing volume of the micelle.

Assuming that any increase in the micellar volume is solely due to the uptake of CO_2 into the core, the aggregation number increases from 53 at atmospheric pressure to 63 at a CO_2 pressure of 50 MPa. The larger aggregation number reported here is a characteristic of the larger micelles observed. An aggregation number of 44 for F127 micelles at 40°C has previously been reported by Rassing *et al.*[57] and an aggregation number of 35 for F127 micelles under similar conditions by Nagarajan[58].

Swelling of F127 Micelles with Propane and Ethane. Figures 2(a) and 2(b) show both the experimental and modelled SANS data from propane and ethane swollen micellar solutions of F127 as a function of pressure. The SANS patterns obtained from the ethane swollen micelles have a more pronounced peak compared to those obtained when using propane as the solvent, indicating a greater interaction between the neighboring micelles during the ethane experiments. It is worth noting that above approximately 5 MPa ethane becomes supercritical.

It has been reported that heavier hydrocarbons are more soluble in PPO relative to lighter hydrocarbons[59] and this observation is reflected in Figures 3(a) and 3(b), which show the modelled micellar radii and the volume fraction of ethane and propane in the cores of the F127 micelles respectively. The greater swelling with propane may also be due to the greater density of propane[60] compared ethane[61] at the experimental pressures.

Figure 3(b) shows the differences in hydrocarbon uptake in the core of the F127 micelles, where a greater uptake of propane into the core is seen relative to ethane. As with the CO_2 experiments,

there is an increase in the aggregation number in both the ethane and propane experiments as the micelle volume increases with pressure, *i.e.* from 53 at atmospheric pressure to an aggregation number of 57 at 30 MPa during the propane experiments and from 53 at atmospheric pressure to an aggregation number of 54 at 30 MPa during the ethane experiments. The addition of hydrocarbon additives to the micellar solutions causes an increase in the volume of the micelles which is accommodated by an increase in the aggregation number.

Temperature Dependent Swelling of F127 Micelles. SANS data was collected from F127 micellar solutions over the temperature range between 40 and 60° C at atmospheric pressure and at a constant pressure of 20 MPa for ethane, propane and heptane solvents at all temperatures. Figures 4(a) to (c) show the changes in the SANS scattering profiles of the F127 micellar solutions as a function of temperature at constant pressure. Initial values of the volume fraction of PPO and water in the micellar cores were determined from experiments conducted in the absence of any swelling solvent as a function of temperature, under atmospheric conditions. The data obtained from these experiments were used in the pressurized hydrocarbon temperature experiments, where we assumed that the addition of a hydrocarbon environment to the micellar solution would not alter the degree of hydration of the micelle core or corona.

The temperature experiments conducted in the absence of any swelling solvent resulted in well known characteristics of a Pluronic micelle solution at different temperatures, most notable an increase in the aggregation number with increasing temperature, but with very little change in micelle size[62], and an increase in the volume fraction of PPO in the core of the micelles as the volume fraction of water in the core decreases. The decreasing volume fraction of water in the

PPO core is due to the lower solubility of water in PPO at higher temperatures[63]. The micelle volume fraction is also seen to decrease slightly after 40 °C, which has also been observed in previous studies[56] and can be attributed to the decrease in the micellar volume as water is lost from the core and corona due to the dehydration of the PEO and PPO segments at elevated temperatures.

Figure 5(a) details the insignificant change in the core radius (R_1) of the F127 micelles as a function of temperature, under atmospheric conditions and in ethane, propane and heptane environments. The initial values of R_1 under different solvent environments are different, within experimental error of the model. The mean core radius R_1 is larger for the heavier hydrocarbon solvents, *i.e.* 49 Å for ethane compared to 50.5 Å for heptane, which can be attributed to the different degree of hydrocarbon solubility in the PPO core. From previous studies on which the Pluronic model here is based, the error associated with the core radius is small and in the order of ±0.5 Å[62] (the error for the aggregation number is ± 1 from the same reference). King *et al.*[54] previously showed that the solubility of propane in a Pluronic micellar solution was greater than that of ethane due to the dominant dispersion forces experienced by the heavier hydrocarbons which dictate the solvent-solute interaction of the system. This solubility trend is reflected in the R_1 values obtained for propane and heptane compared to ethane in our experiments. The volume fraction of hydrocarbon in the core of the F127 micelles at each temperature was also calculated and was found to decrease in the following order, C_7H_{16}>C_3H_8>C_2H_6, which again mirrors the solubility of the various hydrocarbons in the Pluronic micelles. Figure 5(b) shows the increasing aggregation number of the F127 micelles as the temperature is increased, the larger micelles having the greater aggregation number.

CO_2 Swelling of CTAB Micelles. The influence of CO_2 on the structural properties of 2.5 wt% CTAB micellar solutions at 40° C was also investigated by SANS. SANS measurements were recorded at CO_2 pressures up to 50 MPa. The Hayter-Penfold S(q) ellipsoid model, described in the Supporting Information section, was successfully used to fit the SANS data from the swollen CTAB micelles as shown in Figure 6. The volume fraction of the CO_2 could not be refined using this model, but the fact that the swelling seen by CO_2 was so minimal then any changes in the SLD of the CTAB core with the incorporation of CO_2 would also be minimal.

Figure 6 shows the changing neutron scattering from the CTAB micellar solutions as the CO_2 pressure is increased. The pronounced correlation peak illustrates the strong repulsive interactions experienced between the positively charged CTAB micelles.

Table 1 lists some CTAB micelle dimensions obtained from fitting the SANS data shown in Figure 6. The size of the semi-minor (a=b<c for a prolate ellipse) axis reported here 23 Å, which is in agreement with Aswal *et al.*[23]. The shape of the micelle remains that of a prolate ellipsoid up to a CO_2 pressure of 50 MPa. The size of the micelle remains effectively unchanged as does the resulting aggregation, which reflects the very limited uptake of CO_2 into the $C_{16}H_{33}$ core. Very minimal swelling of CTAB with CO_2 was also observed in previous studies, where the swelling of a CTAB templated liquid crystal was also noted to be minimal[41].

The Hayter-Penfold *S(q)* sphere radius (H-P S(q) radius) also remained constant throughout this series of experiments, as did the charge on each micelle and the inverse Debye screening length.

The constant Debye screening length is not surprising given that no electrolyte was added to the micellar solution during the experiments. The inverse Debye screening length was calculated from Griffiths *et al.*[52] and refined during the modelling process, however the value of the inverse Debye screening length changed very little during modelling. The fractional charge (charge per micelle/aggregation number) was determined to be 0.144 at 0.1 MPa and had an average of 0.146 over all pressures. The micelle dimensions quoted in Table 1 have been determined to be typically of the size, shape and nature of CTAB micelles in a dilute aqueous solution[51, 64].

Swelling of CTAB Micelles with Propane. The effect that liquid propane pressure has on the size, shape and characteristics of CTAB micelles was also investigated. A very different response was noted from the CTAB micelles when swollen with propane compared to CO_2. Figure 7 shows the application of the same model (Hayter-Penfold S(q) ellipsoid model) to a 2.5 wt% aqueous CTAB solution under varying liquid propane pressures at 40°C. The correlation peak intensity again indicates the strong repulsive interactions felt between neighboring micelles. The fitted results obtained for this series of experiments are shown in Table 2.

From the data shown in Table 2, propane is observed to have a more substantial effect on the CTAB micelles than CO_2. The increase in the size of the CTAB micelles is a reflection of the high solubility of propane in the C_{16} alkane core of the micelles compared to CO_2. Even though Hayduk *et al.*[65] showed the higher solubility of CO_2 in hexadecane over propane, Roy *et al.*[66] predicated the solubility of a number of non-polar gases including CO_2 and propane in both SDS and CTAB, and reported that the solubility of propane was greatest in both the CTAB and SDS micellar solutions and decreased in the order of propane > ethane > CO_2 > methane.

The SLD of the CTAB core ($C_{16}H_{34}$) and that of propane are very similar (-3.51E-07 $Å^{-2}$ and -2.72E-08 $Å^{-2}$ respectively) so any changes in the CTAB core with the uptake propane would small when measured by SANS. The fact that the amount of propane within the micelle cannot be resolved, means that the increase in the aggregation number of the swollen micelles cannot be determined.

The other micelle characteristics quoted in Table 2 also describe the swelling of the CTAB micellar process which takes place as the propane pressure is increased. The shape of the micelles remains that of a prolate ellipse throughout the whole range of pressures with only a slight decrease in the ellipicity value, which may be due to changes in fractional charge on the micelles as the pressure is increased.

The experiments also highlight the increase in the charge per micelle and the fractional charge as a result of the greater size of the charged micelles. The addition of pressurized propane to the CTAB micellar solution is not thought to have the same neutralising effect that say KBr had in the experiments reported Goyal *et al*. Berr *et al.*[67] proposed that as the ellipitical axial ratio decreases there are less bound counter ions at the micelle interface, *i.e.* counter ion dissociation is promoted, and the head groups move further apart which may be occurring here as the CTAB micelles become more spherical with increasing propane pressure.

This increased micelle surface charge may also be responsible for the narrowing of the correlation peak in the neutron scatting pattern as micelles with greater surface charge repulse neighboring micelles to a greater extent.

Conclusions

Successful modelling of the SANS data from micellar solutions of F127 and CTAB surfactants using well established models, revealed important details of swelling processes occurring at evaluated pressures and temperatures. Not only was the size of the micelles observed to change but the composition of the micelle was also seen to vary as different swelling solvents were incorporated into the core of each micelle. The compositions of the Pluronic micelle was refined during the modelling process and illustrated the increasing volume fraction of swelling solvent, be it CO_2 or propane, within the core of the micelle. The importance of the solubility of each swelling solvent within the PPO core of the micelle was seen to be the driving force for micellar swelling. The effect of changing temperature on a micelle solution, already well characterized, was complicated by the addition of a high pressure environment to the system. The dual processes of pressure and temperature effects occurring simultaneously were both taken into account when the neutron scattering data was modelled. The interaction between neighbouring micelles was influenced greatly by the conditions each system was placed under. Modelling of the ionic CTAB solution also showed interesting results. Not only was the size of the CTAB micelle investigated but also the shape of the micelle was seen to change with varying pressures.

Acknowledgements

The authors acknowledge financial support from the Centre for Research on Adaptive Nanostructures and Nanodevices (CRANN) (Project PR22) and from the European Community through its Access to Research Infrastructure action of the Improving Human Potential Programme.

References

1. Burapatana, V.; Booth, E. A.; Prokop, A.; Tanner, R. D. *Ind. Eng. Chem. Res* **2005,** *44*, 4968.
2. Kristiansen, T. B.; Hagemeister, J. J.; Grave, M.; HellungLarsen, P. *J. Cell. Physi.* **1996,** *169*, 139.
3. Chen, W. J.; Peng, J. M.; Su, Y. L.; Zheng, L. L.; Wang, L. J.; Jiang, Z. Y. *Sep. Purif. Methods* **2009,** *66*, 591.
4. Miksik, I.; Deyl, Z. *J. Chromatogr. B* **2000,** *739*, 109.
5. Oh, K. T.; Bronich, T. K.; Bromberg, L.; Hatton, T. A.; Kabanov, A. V. *J. Control. Release* **2006,** *115*, 9.
6. Sek, L.; Boyd, B. J.; Charman, W. N.; Porter, C. J. H. *J. Pharm. Pharmacol.* **2006,** *58*, 809.
7. Shaik, M. S.; Haynes, A.; McSween, J.; Ikediobi, O.; Kanikkannan, N.; Singh, M. *J. Aerosol Med.* **2002,** *15*, 261.
8. Wei, Z.; Hao, J. G.; Yuan, S.; Li, Y. J.; Juan, W.; Sha, X. Y.; Fang, X. L. *Int. J. Pharm.* **2009,** *376*, 176.
9. Wang, Y. Z.; Li, Y. J.; Zhang, L. J.; Fang, X. L. *Arch. Pharmacal Res.* **2008,** *31*, 530.
10. Sharma, P. K.; Reilly, M. J.; Bhatia, S. K.; Sakhitab, N.; Archambault, J. D.; Bhatia, S. R. *Coll. Surf., B* **2008,** *63*, 229.
11. Alexandridis, P.; Spontak, R. J., *Curr. Opin. Coll. Inter. Sci.* **1999,** *4*, 130.
12. Mortensen, K. *Polym. Adv. Tech.* **2001,** *12*, 2.
13. Zhou, Z. K.; Chu, B. *Macromolecules* **1988,** *21*, 2548.
14. Fujii, S.; Koschoreck, S.; Lindner, P.; Richtering, W. *Langmuir* **2009,** *25*, 5476.
15. Bharatiya, B.; Aswal, V. K.; Bahadur, P. *Pramana J. Phys.* **2008,** *71*, 1009.
16. Newby, G. E.; Hamley, I. W.; King, S. M.; Martin, C. M.; Terrill, N. J. *J. Coll. Inter. Sci.* **2009,** *329*, 54.
17. Bharatiya, B.; Aswal, V. K.; Hassan, P. A.; Bahadur, P. *J. Coll. Inter. Sci.* **2008,** *320*, 452.
18. Han, S.; Hou, W.; Dang, W.; Xu, J.; Hu, J.; Li, D. *Mater. Lett.* **2003,** *57*, 4520.
19. Kim, W. J.; Yang, S. M. *Chem. Mater.* **2000,** *12*, 3227.
20. Moon, S. Y.; Kusunose, T.; Sekino, T. *Mater. Lett.* **2009,** *63*, 2038.
21. Kotkata, M. F.; Masoud, A. E.; Mohamed, M. B.; Mahmoud, E. A. *Physica E* **2009,** *41*, 1457.
22. Zhou, Y. B.; Chen, L.; Hu, X. M.; Lu, J. *Water Sci. Technol.* **2009,** *59*, 957.
23. Aswal, V. K.; Goyal, P. S. *Chem. Phys. Lett.* **2002,** *357*, 491.
24. Aswal, V. K.; Goyal, P. S. *Phys. Rev. E: Stat. Nonlinear Soft Matter Phys.* **2000,** *61*, 2947.
25. Hai, M. T.; Han, B. X. *J. Coll. Inter. Sci.* **2003,** *267*, 173.
26. Chaiko, M. A.; Nagarajan, R.; Ruckenstein, E. *J. Coll. Inter. Sci.* **1984,** *99*, 168.
27. Ma, J. H.; Wang, Y.; Guo, C.; Liu, H. Z.; Tang, Y. L.; Bahadur, P., *J. Phys. Chem. B* **2007,** *111*, 11140.
28. ChilluraMartino, D.; Triolo, R.; McClain, J. B.; Combes, J. R.; Betts, D. E.; Canelas, D. A.; DeSimone, J. M.; Samulski, E. T.; Cochran, H. D.; Londono, J. D. *J. Mol. Struct.* **1996,** *383*, 3.
29. Friman, R.; Rosenholm, J. B. *Coll. Polym. Sci* **1982,** *260*, 545.

30. Lenaerts, V.; Triqueneaux, C.; Quarton, M.; Riegfalson, F.; Couvreur, P. *Int. J. Pharm.* **1987,** *39*, 121.
31. Liu, D. X.; Zhang, J. L.; Han, B. X.; Fan, J. F.; Mu, T. C.; Liu, Z. M.; Wu, W. Z.; Chen, J. *J. Chem. Phys.* **2003,** *119*, 4873.
32. Hakoda, M.; Shiragami, N.; Enomoto, A.; Nakamura, K. *Bioprocess Biosyst. Eng.* **2003,** *25*, 243.
33. Cao, L. A.; Man, T.; Kruk, M. *Chem. Mater.* **2009,** *21*, 1144.
34. Ruggles, J. L.; Gilbert, E. P.; Holt, S. A.; Reynolds, P. A.; White, J. W. *Langmuir* **2003,** *19*, 793.
35. Zhou, X. F.; Qiao, S. Z.; Hao, N.; Wang, X. L.; Yu, C. Z.; Wang, L. Z.; Zhao, D. Y.; Lu, G. Q. *Chem. Mater.* **2007,** *19*, 1870.
36. Causse, J.; Lagerge, S.; de Menorval, L. C.; Faure, S. *J. Coll. Inter. Sci.* **2006,** *300*, 713.
37. Chen, D. H.; Li, Z.; Wan, Y.; Tu, X. J.; Shi, Y. F.; Chen, Z. X.; Shen, W.; Yu, C. Z.; Tu, B.; Zhao, D. Y. *J. Mater. Chem.* **2006,** *16*, 1511.
38. Fukuoka, A.; Kikkawa, I.; Sasaki, Y.; Shimojima, A.; Okubo, T. *Langmuir* **2009,** *25*, 10992.
39. Blin, J. L.; Otjacques, C.; Herrier, G.; Su, B. L. *Langmuir* **2000,** *16*, 4229.
40. O'Driscoll, B. M. D.; Hawley, A. M.; Edler, K. J. *J. Coll. Inter. Sci.* **2008,** *317*, 585.
41. O'Callaghan, J. M.; Copley, M. P.; Hanrahan, J. P.; Morris, M. A.; Steytler, D. C.; Heenan, R. K.; Staudt, R.; Holmes, J. D. *Langmuir* **2008,** *24*, 6959.
42. Hanrahan, J. P.; Copley, M. P.; Ziegler, K. J.; Spalding, T. R.; Morris, M. A.; Steytler, D. C.; Heenan, R. K.; Schweins, R.; Holmes, J. D. *Langmuir* **2005,** *21*, 4163.
43. Eastoe, J.; Paul, A.; Downer, A.; Steytler, D. C.; Rumsey, E. *Langmuir* **2002,** *18*, 3014.
44. Christen, W.; Rademann, K.; Even, U. *J. Chem. Phys.* **2006,** *125*, 5.
45. Horstmann, S.; Fischer, K.; Gmehling, J. *Aiche Journal* **2002,** *48*, 2350.
46. Ewing, M. B.; Ochoa, J. C. S. *J. of Chem. Eng. Data* **2005,** *50*, 1543.
47. Mortensen, K. *J. Phys. Conden. Matter* **1996,** *8*, A103.
48. Yang, L.; Alexandridis, P.; Steytler, D. C.; Kositza, M.; Holzwarth, J. F. *Langmuir* **2000,** *16*, 8555.
49. Goldmints, I.; Yu, G. E.; Booth, C.; Smith, K. A.; Hatton, T. A. *Langmuir* **1999,** *15*, 1651.
50. Heenan, R. K. *FISH Data Analysis Program*; Rutherford Appleton Laboratory Report RAL 89-129: Didcot, U.K., 1989.
51. Quirion, F.; Magid, L. J. *J. Phys. Chem.* **1986,** *90*, 5435.
52. Griffiths, P. C.; Paul, A.; Heenan, R. K.; Penfold, J.; Ranganathan, R.; Bales, B. L. *J. Phys. Chem. B* **2004,** *108*, 3810.
53. Span, R.; Wagner, W. *J. Phys.Chem. Ref. Data* **1996,** *25*, 1509.
54. King, A. D. *J. Coll. Inter. Sci.* **2001,** *244*, 123.
55. Sato, Y.; Takikawa, T.; Yamane, M.; Takishima, S.; Masuoka, H. *Fluid Phase Equilib.* **2002,** *194*, 847.
56. Mortensen, K.; Talmon, Y. *Macromolecules* **1995,** *28*, 8829.
57. Rassing, J.; Attwood, D. *Int. J. Pharm.* **1982,** *13*, 47.
58. Nagarajan, R. *Colloids Surf., B* **1999,** *16*, 55.
59. King, A. D. *J. Coll. Inter. Sci.* **2001,** *243*, 457.
60. Miyamoto, H.; Watanabe, K. *Int. J. Thermophys.* **2000,** *21*, 1045.
61. Friend, D. G.; Ingham, H.; Ely, J. F. *J. Phys. Chem. Ref. Data* **1991,** *20*, 275.

62. Yang, L.; Alexandridis, P.; Steytler, D. C.; Kositza, M. J.; Holzwarth, J. F. *Langmuir* **2000,** *16*, 8555.
63. Goldmints, I.; vonGottberg, F. K.; Smith, K. A.; Hatton, T. A. *Langmuir* **1997,** *13*, 3659.
64. Pal, O. R.; Gaikar, V. G.; Joshi, J. V.; Goyal, P. S.; Aswal, V. K. *Langmuir* **2002,** *18*, 6764.
65. Hayduk, W.; Walter, E. B.; Simpson, P. *J. Chem. Eng. Data* **1972,** *17*, 59.
66. Roy, S.; Mehra, A.; Bhowmick, D. *J. Coll. Inter. Sci.* **1997,** *196*, 53.
67. Berr, S. S. *J. Phys. Chem.* **1987,** *91*, 4760.

Tables and Figures

Table 1 Fitted micelle characteristics as a function of pressure obtained by the application of the Hayter-Penfold S(Q) ellipsoid model to the 2.5 wt% CTAB scattering data seen in Figure 6.

	0.1 MPa	**5 MPa**	**20 MPa**	**30 MPa**	**50 MPa**
a = b (Å)$^{\alpha}$	23	24	26	26	25
X, *c* = X.a$^{\beta}$	1.65	1.49	1.49	1.48	1.51
H-P *S(q)* Sphere Radius Å$^{\gamma}$	25	24	25	24	23

α: is the semi-minor axis of the ellipitical CTAB micelle

β: is the ellipicity of the CTAB micelle, the closer to unit this figure is the more spherical the micelle becomes

γ: this is the S(Q) hard sphere radius

Table 2. The results of the modelled micelle scattering observed in Figure 7 at each propane pressure, obtained by application of the Hayter-Penfold S(Q) ellipsoid model to the 2.5 wt% CTAB scattering data.

	0.1 MPa	**0.6 MPa**	**1.2 MPa**	**4.7 MPa**	**10 MPa**	**25 MPa**	**50 MPa**
a = b (Å)$^{\alpha}$	23	26	34	34	35	34	34
X, *c* = X.a$^{\beta}$	1.65	1.49	1.47	1.47	1.46	1.46	1.47
H-P *S(q)* Sphere Radius Å$^{\gamma}$	25	23	29	29	30	28	28

α: is the semi-minor axis of the ellipitical CTAB micelle

β: is the ellipicity of the CTAB micelle, the closer to unit this figure is the more spherical the micelle becomes

γ: this is the S(Q) hard sphere radius

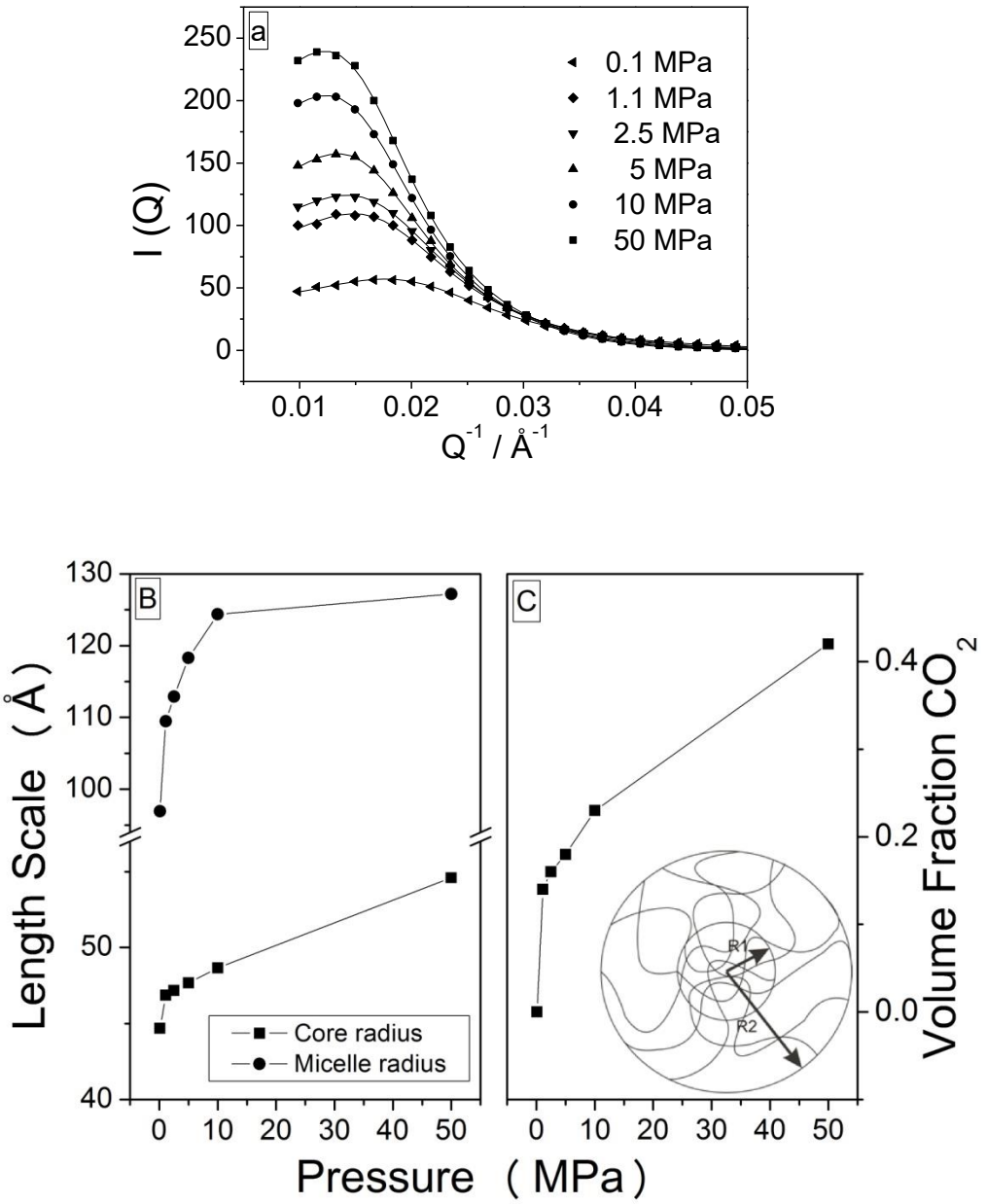

Figure 1. (a) SANS data for a 2.5wt% F127 aqueous micellar solution under various CO_2 pressures at 40 °C, collected data (square dots) and fitted data (solid line), (b) the resulting micelle characteristics obtained from the fitted data shown in (a). Shown are the core radius R_1 and the micelle radius R_2. (c) Fitted CO_2 volume fractions in the core of the micelles as a function of pressure. Figure inset shows the core radius R_1 and the corona radius R_2.

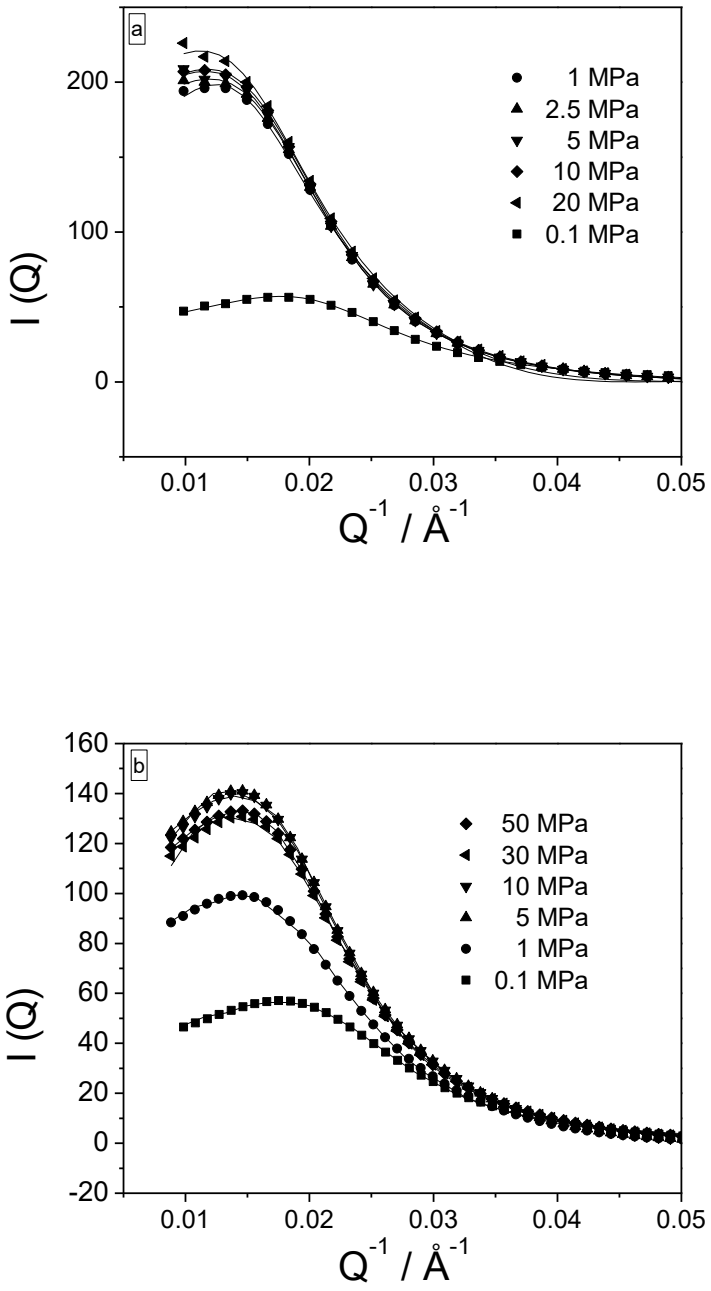

Figure 2. SANS data, for a 2.5 wt% F127 aqueous micellar solution under various (a) propane and (b) ethane pressures, at a temperature of 40 °C. Collected data (square dots) and fitted data (solid line).

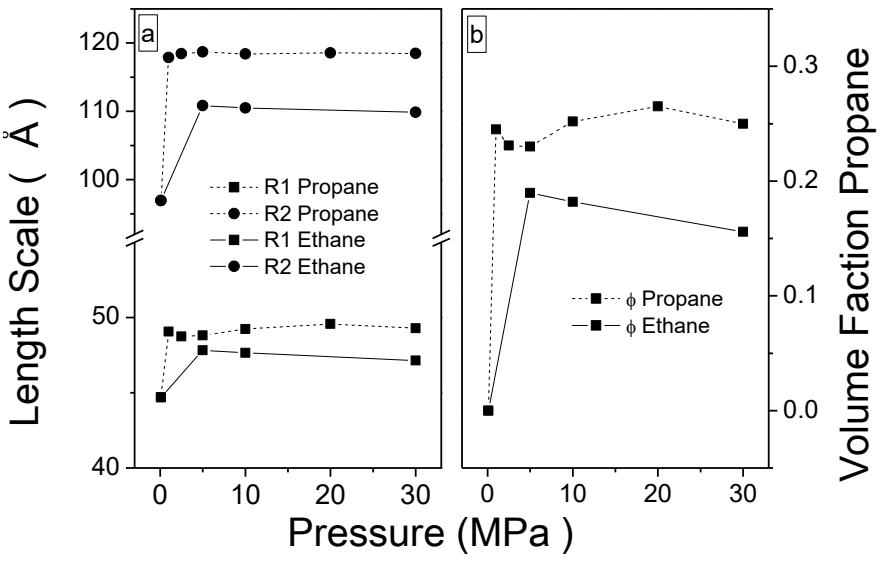

Figure 3. Data showing (a) resulting micelle characteristics obtained from the fitting of the SANS data in Figure 2(a). Shown in (a) is the core radius, R_1 and the micelle radius R_2 of the F217 under various ethane and propane pressures. (b) Volume fraction of hydrocarbon taken up by the F127 micelle at different pressures.

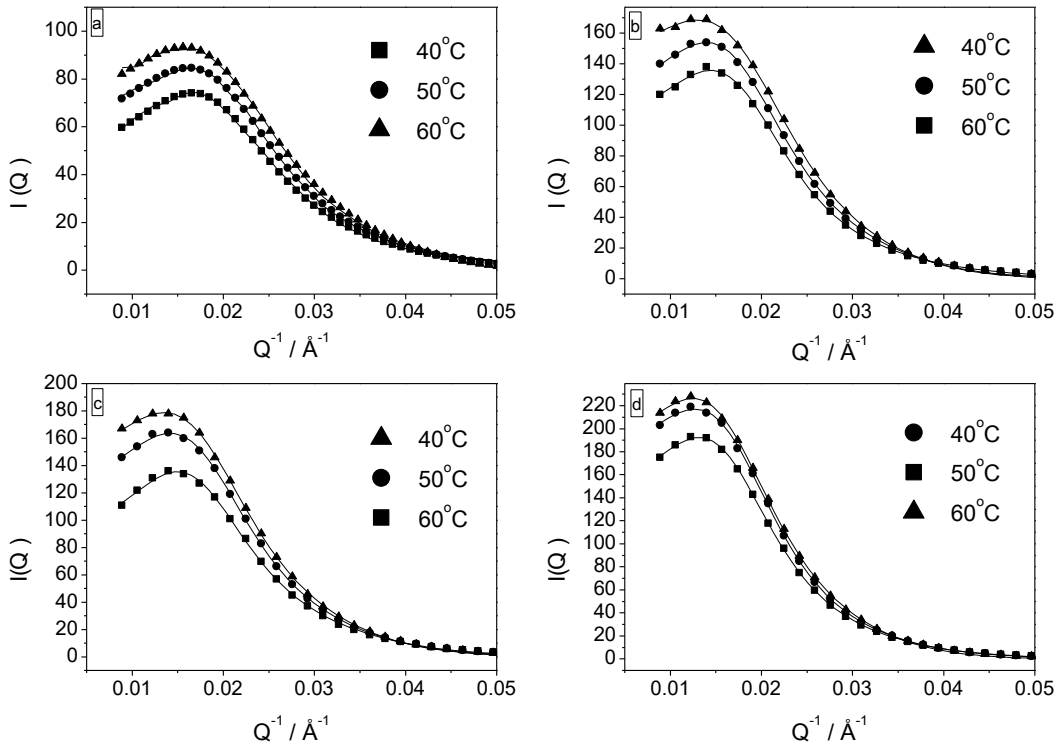

Figure 4. SANS data showing the scattering pattern from the F127 micellar solutions as a function of temperature under (a) atmospheric conditions, (b) 20 MPa ethane pressure, (c) 20 MPa propane pressure and (d) under 20 MPa heptane pressure. Collected data is shown as square dots and the modelled profiles are shown as solid lines.

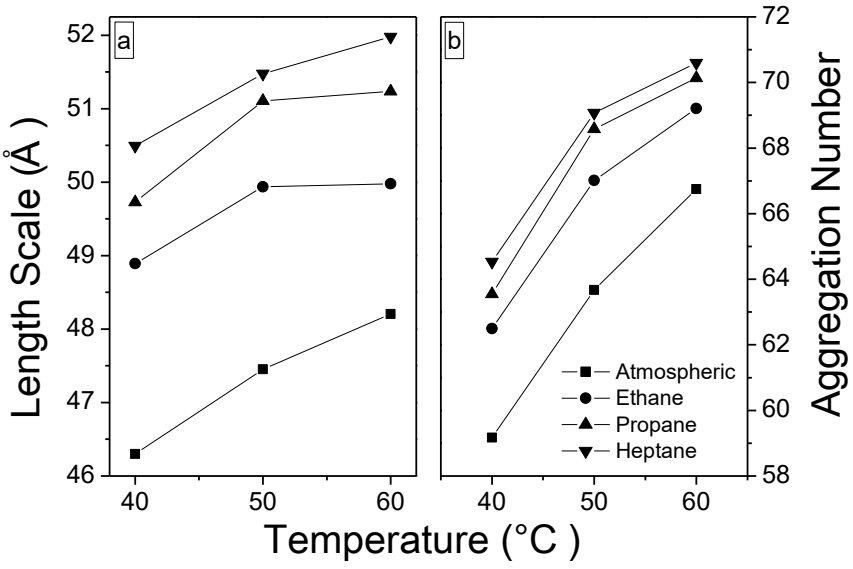

Figure 5. (a) Changes in the core radius the of F127 micelles over the temperature range between 40 to 60 °C, under atmospheric conditions and at a constant ethane, propane and heptane pressures of 20 MPa and (b) changing aggregation number of the micelles at different temperatures. The same legend can be applied to both figures.

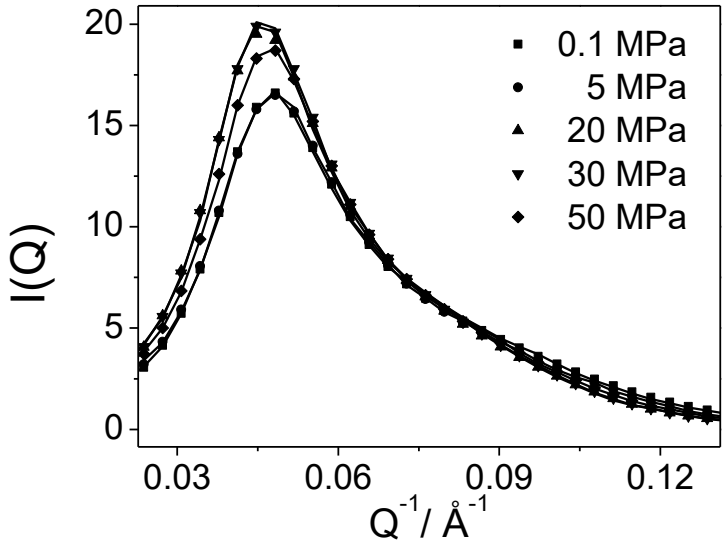

Figure 6. SANS data from CO_2-swollen CTAB micellar solutions at a constant temperature of 40°C (black dots) and modelled scattering data (continuous line).

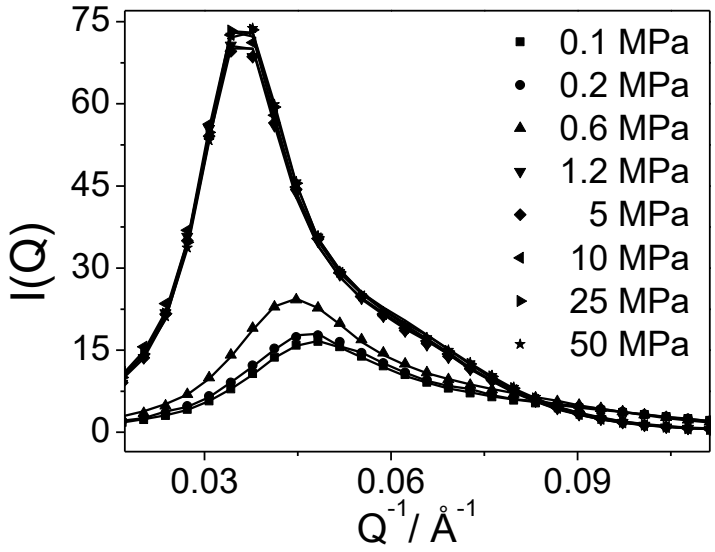

Figure 7. SANS data (dots) and fitted scattering curves (solid lines) for 2.5 wt% aqueous CTAB solutions under varying liquid propane pressure at 40° C.

Table of Contents Figure

Swelling of Ionic and Non-Ionic Surfactant Micelles by High Pressure Gases
John M. O' Callaghan, Hugh McNamara, Mark P. Copley, John P. Hanrahan, Michael A. Morris, David C. Steytler, Richard K. Heenan and Justin D. Holmes